



Thermal Stability for Reflectance and Specific Contact Resistance of Ni/Ag-Based Contacts on p-Type GaN

Ray-Ming Lin,^{a,b,z} Yi-Lun Chou,^c Wan-Ching Tseng,^a Chia-Lung Tsai,^a Jen-Chih Li,^a and Meng-Chyi Wu^c

^aDepartment of Electronic Engineering and ^bGreen Research Technology Center, Chang-Gung University, Taoyuan 33302, Taiwan

^cInstitute of Electronics Engineering and Department of Electrical Engineering, National Tsing-Hua University, Hsinchu 30013, Taiwan

In this study, we investigated the thermal stability of Ni/Ag-based alloy contacts on p-type GaN. We observed the morphology of aggregated Ag for the Ni/Ag bilayer on p-type GaN after annealing it at 500°C in an O₂ ambient. To improve the thermal stability, we deposited a Ni/Ag/Au trilayer onto p-type GaN. In this case, Ag aggregation was retarded after thermal annealing, and the specific contact resistance exhibited improved stability. Furthermore, because strong interdiffusion of the Au and Ag layers leads to poor reflectance, we added a diffusion barrier layer into the system; i.e., we deposited Ni/Ag/Ti/Au onto p-type GaN, with the Ti layer playing the role of the diffusion barrier. After annealing, the contact exhibited diminished Ag aggregation and a lower level of interdiffusion of the Au and Ag layers. We investigated the effect of the annealing time (at 500°C in an O₂ ambient) on the properties of the Ni/Ag (1/150 nm), Ni/Ag/Au (1/150/150 nm), and Ni/Ag/Ti/Au (1/150/500/150 nm) layers, namely, their values of specific contact resistance, determined using a modified transmission line model, and reflectance at 465 nm. According to analyses by using scanning electron microscopy and secondary-ion mass spectrometry, we determined that the aggregation of Ag and the interdiffusion of Au and Ag within the Ni/Ag/Ti/Au construct were both minimized with the presence of the Ti layer, thereby improving the thermal stability of the contact on the p-type GaN.

© 2009 The Electrochemical Society. [DOI: 10.1149/1.3152593] All rights reserved.

Manuscript submitted February 26, 2009; revised manuscript received May 4, 2009. Published June 12, 2009.

Gallium nitride (GaN) and its relative group-III nitrides play important roles in compound semiconductors, especially for those used in optoelectronics devices. At room temperature, the bandgap energy of GaN is 3.4 eV; it forms several alloys having bandgaps ranging from 0.7 (InN) to 6.2 eV (AlN), making it suitable for use in green, blue, and UV light-emitting diodes (LEDs). Because of its excellent electronic, optical, and thermal properties, GaN has become increasingly attractive for practical applications. Future high performance devices will require LEDs possessing thermally stable, high quality contacts to p/n-type GaN-based semiconductors. Because it is difficult to achieve a high carrier concentration of p-type GaN, low contact resistances are rarely obtained. Furthermore, high brightness LEDs require high light extraction efficiencies and high internal quantum efficiencies. Because flip-chip¹ and vertical-structure^{2,3} GaN-based LEDs exhibit superior light extraction and heat-sink effects, they exhibit an enhanced device performance. These two types of LED structures are fabricated by using high reflectance, low contact resistance p-type alloy contacts, such as Ag layers.⁴ Unfortunately, these Ag layers exhibit a poor thermal stability of their reflectance and ohmic contact on p-type GaN as a result of Ag aggregation during thermal annealing.⁵ Several alternative materials have been investigated to obtain reliable Ag-based ohmic contacts on p-type GaN, including Ni/Ag(Al),⁵ Cu-Ni solid solution/Ag,⁶ Ag/Cu,⁷ Ni/Ag/Ru/Ni/Au,⁸ and (Ni/Ag)-annealed/Au.⁹ In this study, we compared the thermal stability for reflectance and ohmic contact of Ni/Ag, Ni/Ag/Au, and Ni/Ag/Ti/Au layers on p-type GaN. Based on our analytical results, we propose a mechanism for the reflective ohmic contact on p-type GaN.

Experimental

Taiyo Nippon Sanso SR2000 metallorganic chemical vapor deposition was used to grow the p-type GaN on a *c*-plane sapphire substrate. Trimethylgallium, trimethylindium, and ammonia (NH₃) were used as sources; biscyclopentadienylmagnesium (CP₂Mg) was the p-type dopant. The structure of the p-type GaN comprised a 30 nm thick GaN buffer layer, a 2 μm thick undoped GaN layer, and a 1 μm thick Mg-doped GaN layer.

After growth, the sample was treated in a quartz furnace for activation under a N₂ ambient. The annealing temperature and time

were 700°C and 30 min, respectively. The carrier concentration of the p-type GaN was $3 \times 10^{17} \text{ cm}^{-3}$, as determined through Hall measurement. The samples were then ultrasonically rinsed with acetone, methanol, and deionized water and then the p-type GaN wafer was dipped into buffered oxide etch solution to remove the native oxide. Contact metals having three structures, Ni/Ag (1/150 nm), Ni/Ag/Au (1/150/150 nm), and Ni/Ag/Ti/Au (1/150/500/150 nm), were deposited in sequence onto the p-type GaN and glass substrate using an electron-beam evaporator under a pressure of 3×10^{-6} Torr. After deposition, the three contact structures were thermally annealed for various lengths of time at 500°C in an O₂ ambient. To measure the specific contact resistance, photolithography techniques were used to pattern a modified transmission line model¹⁰ on the p-type GaN. The reflectance at 465 nm was also measured spectrometrically for the contact metal deposited onto a glass substrate. The three structures of the contact metal were also deposited onto p-type GaN for characterization by using scanning electron microscopy (SEM) and secondary-ion mass spectrometry (SIMS).

Results and Discussion

Figure 1 shows the specific contact resistances of the Ni/Ag (1/150 nm), Ni/Ag/Au (1/150/150 nm), and Ni/Ag/Ti/Au (1/150/500/150 nm) layers on p-type GaN as a function of annealing temperature. The contact resistivities of most contact schemes decreased upon thermal annealing in the temperature range from 300 to 500°C due to increased crystallinity of the metal itself. Furthermore, many researchers showed that the reduction in specific contact resistance in an O₂ ambient has more effect than that in a N₂ ambient. This result indicated that the oxidation annealing is a key factor to obtain the low contact resistance for the Ni/Ag-based contacts on p-type GaN.^{4,5} The minimum contact resistivities of the contacts were obtained at around 500°C. However, at annealing temperature higher than 500°C the contact resistivity increased, showing the degradation of the contact.

Figure 2 displays the specific contact resistances as a function of annealing time at 500°C under an O₂ ambient, evaluating the thermal stability of the three kinds of contacts. For the Ni/Ag contact, the specific contact resistance changed from $4.86 \times 10^{-1} \Omega \text{ cm}^2$ for the as-grown sample to 1.97×10^{-2} , 1.02×10^{-1} , 5.83×10^{-1} , 6.02×10^{-1} , 6.54×10^{-1} , and $6.80 \times 10^{-1} \Omega \text{ cm}^2$ after annealing for 2, 5, 10, 15, 20, and 25 min, respectively. This behav-

^z E-mail: rmlin@mail.cgu.edu.tw

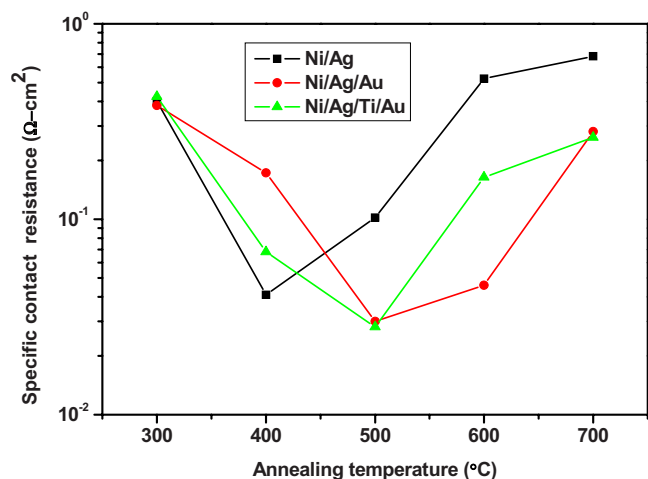


Figure 1. (Color online) Specific contact resistance of all samples as a function of annealing temperature.

ior, an initial decrease then an increase in contact resistance upon increasing the annealing time, was caused by the formation of a Ag–Ga solid solution and the increased surface carrier concentration of p-type GaN that arose as a result of the generation of Ga vacancies during the annealing process.^{4,11,12} When the annealing time was prolonged, the aggregation of Ag deteriorated the thermal stability and increased the specific contact resistance.^{5,13} For the Ni/Ag/Au contact, in contrast, the specific contact resistance changed from $4.98 \times 10^{-1} \Omega \text{ cm}^2$ for the as-grown sample to 2.83×10^{-1} , 3.00×10^{-2} , 1.15×10^{-2} , 1.28×10^{-2} , 1.13×10^{-2} , and $2.60 \times 10^{-2} \Omega \text{ cm}^2$ after annealing for 2, 5, 10, 15, 20, and 25 min, respectively. The Ni/Ag/Au contact layer featured a more stable contact layer, which can be understood in terms of its retardant effect on Ag aggregation. The specific contact resistance remained on the order of $10^{-2} \Omega \text{ cm}^2$ after annealing for 25 min. Finally, for the Ni/Ag/Ti/Au contact, the specific contact resistance changed from $4.58 \times 10^{-1} \Omega \text{ cm}^2$ for the as-grown sample to 4.94×10^{-2} , 2.81×10^{-2} , 1.80×10^{-1} , 2.25×10^{-1} , 2.62×10^{-1} , and $2.44 \times 10^{-1} \Omega \text{ cm}^2$ after annealing for 2, 5, 10, 15, 20, and 25 min, respectively. The Ni/Ag/Ti/Au contact had thermal stability that was superior to that of the Ni/Ag contact. When its annealing time was 5 min, the specific contact resistance decreased to $2.81 \times 10^{-2} \Omega \text{ cm}^2$, but it increased upon increasing the annealing time

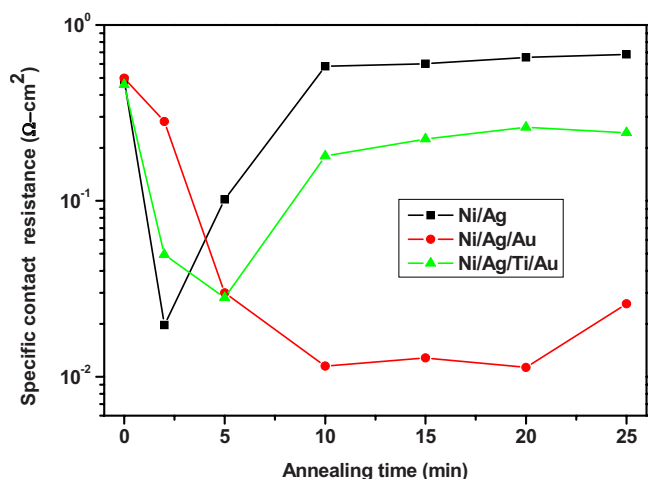


Figure 2. (Color online) Specific contact resistance of Ni/Ag, Ni/Ag/Au, and Ni/Ag/Ti/Au contacts on p-type GaN plotted with respect to the annealing time.

to 20 min. In our experience, when increasing the Ni thickness from 1 to 3 nm in Ni/Ag/Ti/Au contact structure, the specific contact resistance decreased to the order of $10^{-3} \Omega \text{ cm}^2$ (not shown here). Meanwhile, the specific contact resistance was also strongly dependent on the p-contact layer structure and the doping concentration.

Figure 3 displays SEM images of the surfaces of the Ni/Ag, Ni/Ag/Au, and Ni/Ag/Ti/Au layers. The degree of Ag aggregation of the Ni/Ag layer increases upon increasing the annealing time; this behavior leads to the initial decreases in both the reflectance and contact resistivity, and the resulting poor thermal stability then induces increases in contact resistivity and reduced reflectance.^{5,13} For the Ni/Ag/Au layer, Ag aggregation was retarded initially, providing a surface morphology that was smoother than that of the Ni/Ag layer under the same annealing conditions. When we extended the annealing time to 10 min, however, the surface of the Ni/Ag/Au layer became rougher because of partial Ag aggregation and interdiffusion of the Au and Ag layers.¹⁴ Moreover, the surface of the Ni/Ag/Ti/Au layer was even smoother than those of the Ni/Ag and Ni/Ag/Au layers under the same annealing conditions. It was suspected that Ti acted as a diffusion barrier layer, preventing both Ag aggregation and diffusion between Au and Ag. The Ni/Ag/Ti/Au contact structure maintained its smooth surface morphology after 10 min of annealing. Therefore, inserting a Ti layer between the Au and Ag layers is an effective means of diminishing Ag aggregation and interdiffusion.

Figure 4 presents the SIMS depth profiles of the Ni/Ag/Au and Ni/Ag/Ti/Au layers before and after annealing for 10 min at 500°C in an O_2 ambient. For both annealed samples, Ga atoms outdiffused as Ag atoms in-diffused, presumably leading to the formation of Ag–Ga solid solutions, and decreased specific contact resistance because of Ga vacancies. For the Ni/Ag/Au layer, the intermixing of Ni, Ag, and Au atom led to a stable, low contact resistance, but it reduced the light reflection as a result of strong interdiffusion between Au and Ag atoms. For the Ni/Ag/Ti/Au layer, we also observed intermixing of the Ga and Ag atoms, but the Ti layer prevented the Au and Ag layers from interdiffusing, thereby diminishing the reduction in light reflectance.^{8,15}

Figure 5 displays the light reflectance at 465 nm of the Ni/Ag (1/150 nm), Ni/Ag/Au (1/150/150 nm), and Ni/Ag/Ti/Au (1/150/500/150 nm) layer contacts on glass substrates as a function of the annealing time. For the Ni/Ag layer, the reflectance changed from 91.0% for the as-grown sample to 87.6, 67.5, 58.3, 52.4, 50.2, and 47.6% after annealing for 2, 5, 10, 15, 20, and 25 min, respectively. The reflectance decreased upon increasing the annealing time, dropping to 47.6% when the annealing time reached 25 min. The reflectance of the Ni/Ag/Au layer changed from 92.0% for the as-grown sample to 73.6, 12.6, 33.1, 34.2, 32.8, and 28.9% after annealing for 2, 5, 10, 15, 20, and 25 min, respectively; after annealing for 10 min, this behavior is consistent with the evidence for Au and Ag interdiffusion provided in the reported studies^{8,9,14,15} and is supported by the SIMS data, as shown in Fig. 3. Furthermore, the reflectance of the Ni/Ag/Ti/Au layer changed from 92.0% for the as-grown sample to 80.5, 83.8, 91.7, 89.6, 83.5, and 78.8% after annealing for 2, 5, 10, 15, 20, and 25 min, respectively. For the Ni/Ag/Ti/Au layer, the reflectance change with annealing time has a similar trend with the Ni/Ag/Au layer. But, the excellent visible light reflectance of 83.8% was obtained after annealing at 500°C for 5 min in O_2 ambient. This result told us that the Ag layer in the Ni/Ag/Ti/Au (1/150/500/150 nm) contact could act as an effective reflection mirror after the oxidation annealing. Then, the Ti layer plays a role of a diffusion barrier to prevent the interdiffusion of Ag and Au as well as an adhesion layer due to poor adhesion of Ag and Au, resulting in both the high reflectance and excellent thermal stability we observed. The mechanism of the improved reflectance of the Ni/Ag/Ti/Au contact should be investigated further, and the Ni/Ag/Ti/Au contact could be a very suitable metallization scheme for high power flip-chip and vertical-structure GaN-based LEDs.

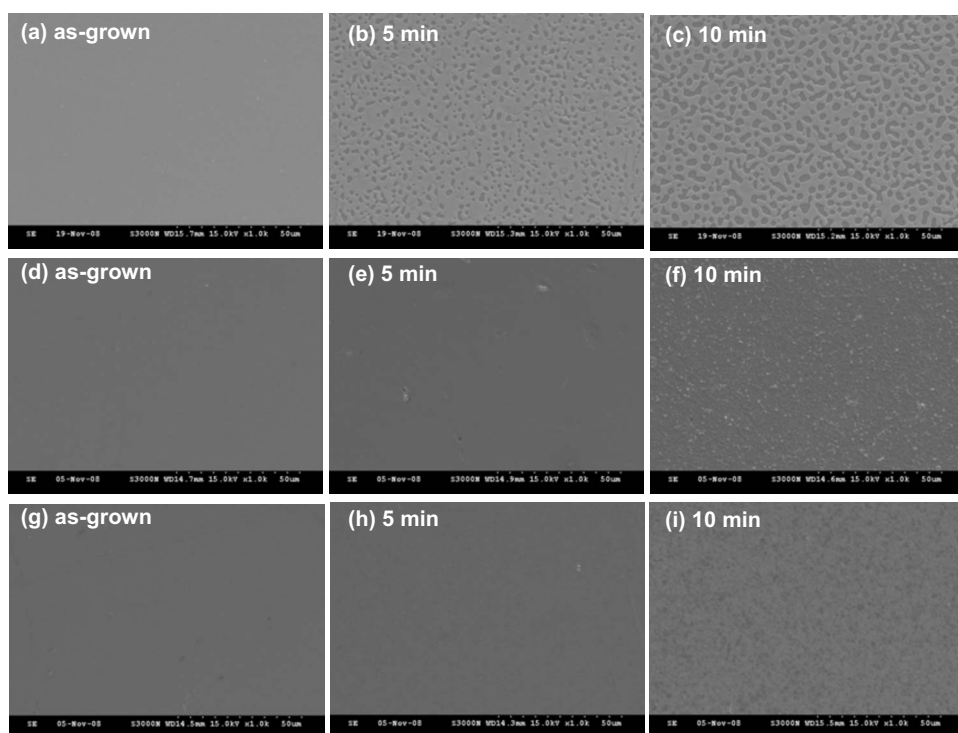


Figure 3. SEM images of the surface of Ni/Ag contact for (a) as grown, (b) 5, and (c) 10 min; Ni/Ag/Au contact for (d) as grown, (e) 5, and (f) 10 min; and Ni/Ag/Ti/Au contact for (g) as grown, (h) 5, and (i) 10 min on p-type GaN before and after annealing at 500°C in an O₂ ambient.

Conclusion

We have been investigated approaches toward improving the thermal stability of the reflectance and specific contact resistance of Ni/Ag-based contacts on p-type GaN. After annealing for 5 min, the specific contact resistances of the Ni/Ag (1/150 nm), Ni/Ag/Au (1/150/150 nm), and Ni/Ag/Ti/Au (1/150/500/150 nm) layers were 1.02×10^{-1} , 3.00×10^{-2} , and $2.81 \times 10^{-2} \Omega \text{ cm}^2$, respectively; their values for the reflectance of light at 465 nm were 67.5, 12.6, and 83.8%, respectively. Thus, the Ti layer in Ni/Ag/Ti/Au (1/150/

500/150 nm) contact provides an effective diffusion barrier layer for Ni/Ag-based contacts on p-type GaN. The Ni/Ag/Ti/Au contact structure is thought suitable for use in flip-chip and vertical-structure GaN-based LEDs.

Acknowledgment

The authors acknowledge the support of National Science Council of Taiwan under contract no. NSC 96-2221-E-182-049-MY3.

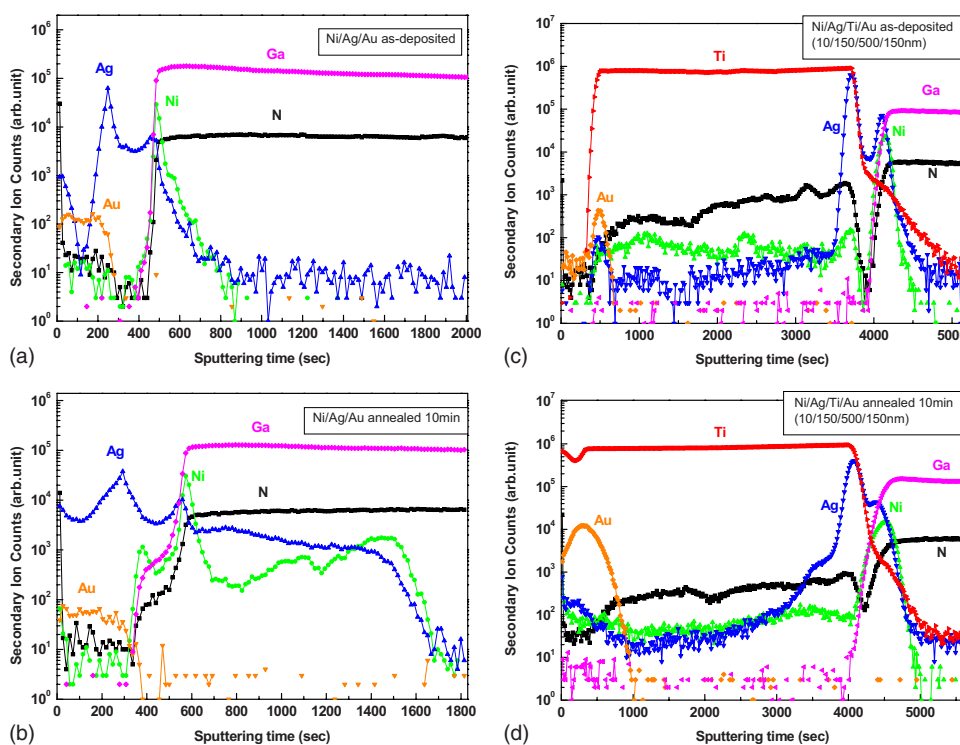


Figure 4. (Color online) SIMS depth profiles of Ni/Ag/Au contact for (a) as grown and (b) 10 min and Ni/Ag/Ti/Au for (c) as grown and (d) 10 min contact on p-type GaN before and after annealing at 500°C in an O₂ ambient.

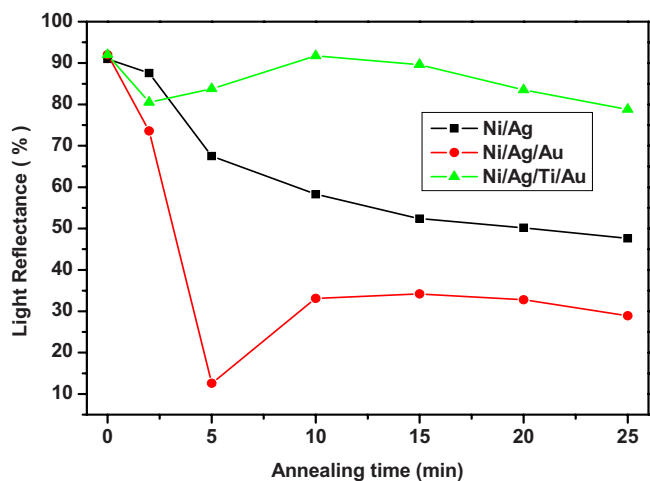


Figure 5. (Color online) Values of the light reflectance at 465 nm of Ni/Ag, Ni/Ag/Au, and Ni/Ag/Ti/Au contacts on glass substrates plotted with respect to the annealing time.

Chang Gung University assisted in meeting the publication costs of this article.

References

1. W. K. Hong, J.-O. Song, H. G. Hong, K. Y. Ban, T. Lee, J. S. Kwak, Y. Park, and T. Y. Seong, *Electrochem. Solid-State Lett.*, **8**, G320 (2005).
2. S. J. Wang, K. M. Uang, S. L. Chen, Y. C. Yang, S. C. Chang, T. M. Chen, C. H. Chen, and B. W. Liou, *Appl. Phys. Lett.*, **87**, 011111 (2005).
3. W. Y. Lin, D. S. Wu, K. F. Pan, S. H. Huang, C. E. Lee, W. K. Wang, S. C. Hsu, Y. Y. Su, S. Y. Huang, and R. H. Horng, *IEEE Photonics Technol. Lett.*, **17**, 1809 (2005).
4. H. W. Jang and J. L. Lee, *Appl. Phys. Lett.*, **85**, 5920 (2004).
5. C. H. Chou, C. L. Lin, Y. C. Chuang, H. Y. Bor, and C. Y. Liu, *Appl. Phys. Lett.*, **90**, 022103 (2007).
6. D. S. Leem, J.-O. Song, J. S. Kwak, Y. Park, and T. Y. Seong, *Electrochem. Solid-State Lett.*, **7**, G210 (2004).
7. H. Kim, K. H. Baik, J. Cho, J. W. Lee, S. Yoon, H. Kim, S. N. Lee, C. Sone, Y. Park, and T. Y. Seong, *IEEE Photonics Technol. Lett.*, **19**, 336 (2007).
8. H. W. Jang and J. L. Lee, *Appl. Phys. Lett.*, **85**, 4421 (2004).
9. L. B. Chang, C. C. Shiu, and M. J. Jeng, *Appl. Phys. Lett.*, **90**, 163515 (2007).
10. N. C. Chen, C. Y. Tseng, A. P. Chiu, C. F. Shih, and P. H. Chang, *Appl. Phys. Lett.*, **85**, 6086 (2004).
11. J.-O. Song, J. S. Kwak, Y. Park, and T. Y. Seong, *Appl. Phys. Lett.*, **86**, 062104 (2005).
12. J.-O. Song, H. G. Hong, J. W. Jeon, J. I. Sohn, J. S. Jang, and T. Y. Seong, *Electrochem. Solid-State Lett.*, **11**, H36 (2008).
13. S. Kim, J. H. Jang, and J. S. Lee, *J. Electrochem. Soc.*, **154**, H973 (2007).
14. C. L. Chang, Y. C. Chuang, and C. Y. Liua, *Electrochem. Solid-State Lett.*, **10**, H344 (2007).
15. S. Y. Kim and J. L. Lee, *Electrochem. Solid-State Lett.*, **7**, G102 (2004).